

9-25-1993

## Mechanisms of Cavity Growth During Ion Implantation

J. H. Evans  
*University of London*

Follow this and additional works at: <https://digitalcommons.usu.edu/microscopy>



Part of the [Biology Commons](#)

---

### Recommended Citation

Evans, J. H. (1993) "Mechanisms of Cavity Growth During Ion Implantation," *Scanning Microscopy*. Vol. 7 : No. 3 , Article 8.

Available at: <https://digitalcommons.usu.edu/microscopy/vol7/iss3/8>

This Article is brought to you for free and open access by the Western Dairy Center at DigitalCommons@USU. It has been accepted for inclusion in Scanning Microscopy by an authorized administrator of DigitalCommons@USU. For more information, please contact [digitalcommons@usu.edu](mailto:digitalcommons@usu.edu).



## MECHANISMS OF CAVITY GROWTH DURING ION IMPLANTATION

J.H. Evans

Physics Department, Royal Holloway, University of London,  
Egham, Surrey, TW20 0EX, England

Present address: 27 Clevelands, Abingdon, Oxon., OX14 2EQ, England

Telephone number: +44-235-525059

(Received for publication May 9, 1993, and in revised form September 25, 1993)

### Abstract

This paper will review two separate areas of cavity growth under ion implantation, firstly bias-driven void growth occurring in metals over the range 0.3 to 0.5 of the melting point at high displacement doses, and secondly, bubble growth during inert gas implantation. Interesting phenomena take place in both areas, e.g. void swelling and void lattice formation in the first and blistering, bubble lattices and the precipitation of heavier inert gases in the solid phase in the second. These phenomena will be described together with the extension of mechanisms to other implant species such as carbon where the possibility of precipitation in the diamond phase might be of interest.

### Introduction

The aim of this paper is to give a brief overview of the more interesting phenomena occurring in the title area. However, one has to distinguish two distinct areas of cavity growth in metals, firstly that of void growth where the cavity within the metal is essentially empty, and secondly that of bubble growth where the cavity is essentially full of inert gas. (The meaning of 'full' in this context will become apparent later). As will be explained, the growth processes of cavities in the two cases are different, with displacement damage being the dominant feature for void growth, and the inert gas itself the driving force for bubble growth.

For both phenomena, ion beam studies have been very useful. Transmission electron microscopy (TEM) has been the dominant method of study for small cavities in metals but in studies of inert gas behaviour there have been valuable contributions from scanning electron microscopy (SEM). This paper makes only marginal references to the many other techniques in this wide field: the main emphasis is on the general qualitative understanding of the underlying mechanisms controlling the observed phenomena.

### Void Growth

In 1966, the examination of the stainless steel cladding material around fuel pins taken from the Dounreay Fast Reactor in Scotland showed that considerable swelling of the material had occurred after prolonged neutron irradiation. Further studies on this material using TEM were carried out by Cawthorne and Fulton (1966) who demonstrated that it contained a concentration of small cavities with diameters in the tens of nanometers range. While the formation of cavities due to inert gas precipitation was already known (see later in this paper), it was realised that although some helium would be present from  $(n,\alpha)$  reactions, there was far from sufficient gas to explain the measured cavity swelling. As a result, these cavities were described as voids and the term void swelling introduced. An example of void formation is shown in Fig.1, illustrating the substructure of vanadium after neutron irradiation.

**Key Words:** Metals, radiation damage, displacement damage, void formation, ion implantation, bubbles, solid krypton, void lattices, void swelling, inert gas precipitation.

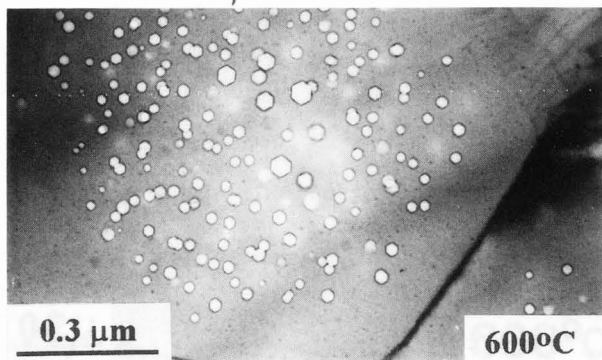


**Figure 1.** Transmission electron micrograph of voids formed in vanadium neutron irradiated at 600°C to a dose of  $\sim 35$  displacements per atom.

The Cawthorne-Fulton observations were the start of a major field of investigation with many hundreds of subsequent publications, both experimental and theoretical. There was a very strong technical case for work on void swelling since the discovery was made at a time when plans and designs for commercial fast reactors were proceeding with considerable impetus. The formation and growth of voids, and the commensurate void swelling, in metal components such as cladding, wrappers and the fuel assemblies gave a number of potential problems which had to be addressed and understood. As a result, the area was discussed in considerable depth at international conferences in the early '70s (Corbett and Ianniello, 1972; Pugh et al., 1971). Although studies were continued under the umbrella of the fast reactor, later work, even up to the present, has examined the topic from the point of view of fusion technology, particularly that of the first wall; a number of fusion technology conferences (Nygren et al., 1981; Ishino et al., 1991) contain relevant papers. The field is so large that even a partial review would be well beyond the scope of the present paper, but an attempt to cover the essential elements will be made.

#### Displacement Damage

It was recognised at an early stage that the displacement damage produced by the high dose neutron irradiation was the first key element in void swelling. As is well known, the transfer of momentum from fast neutrons can displace the host atom - giving a primary knock-on - which, if its energy is high enough, can in turn displace further host atoms, i.e. secondary knock-ons. The simple picture is the production of a cascade of damage with a core of vacancies collapsing to give a vacancy loop and a population of vacancies, interstitials and interstitial loops at the periphery. However, an outline account of void swelling need only consider the free vacancies and interstitials since voids are found under high energy electron irradiation when cascades are not formed.

Nevertheless, it is important to recognise the main facets of displacement cascades since normally they are present and, as will be seen, can influence the void growth parameters. The exact behaviour of atoms in a displacement case is still attracting interest, with several recent studies using computer molecular dynamics programs (Diaz de la Rubia and Guinan, 1991, Foreman et al., 1992). For void swelling, the second key element is that some vacancy clusters are in a three dimensional form, the collapse to the lower energy loop form being prevented by gas atoms, e.g. the (n, $\alpha$ ) helium atoms. However, other atoms can have the same effect, one of the best examples being that of added oxygen on void nucleation in tantalum and niobium in the work of Loomis et al. (1977). These three-dimensional vacancy clusters have the potential to be void nuclei and are the starting point for discussing the mechanism of void growth.

#### Mechanism of Void Growth

It is self-evident that the growth of voids must be due to the capture of vacancies. The question is how the voids acquire more vacancies than interstitials. An interesting feature of the void story is that the generally accepted mechanism, the so-called bias-driven mechanism, was suggested as a possibility by Greenwood et al., (1959) several years before the observation of voids. In this mechanism, the driving force for void growth comes from the strain field interaction of dislocations with the interstitial component of the displacement damage. This gives the dislocations a slight 'bias' for interstitials and results in the fraction of interstitials captured in unit time by dislocations to be slightly greater than that of vacancies, thus leaving an equivalently larger flux of vacancies to be captured by other sinks, including void nuclei. These, to a first approximation, can be considered to be 'neutral' sinks. Therefore they must acquire more vacancies than interstitials, leading to void growth. (Recently, the role of a production bias, involving the clustering of interstitials in the cascade event, has been proposed (Woo and Singh, 1992) but this will not be considered here).

Some basic equations can be derived to show the dependence of void growth on the relative sink strengths of voids and dislocations. However, it is first worth pointing out some of the complications that can affect the simple picture given above, particularly those that affect the temperature range of void formation in metals. Clearly, vacancy mobility is a prerequisite for void growth but for fcc metals at least, the lower temperature bound for irradiation conditions in which cascades are created is controlled by the collapse of vacancy loops within the cascade. Below about 0.3 of the metal melting point,  $T_m$ , this collapse will remove a fraction of vacancies from the number available to freely migrate through the substructure, thus inhibiting any void growth. Through the 0.3  $T_m$  temperature range, the vacancy loops become increasingly thermally unstable and their effect is then

removed. The next significant temperature is at around  $0.5 T_m$  at which temperature the voids themselves become unstable and emit vacancies back to the system. The equation covering this process is left until the discussion later in this paper on high temperature bubble effects where it also applies. The essentials of the above mechanism are illustrated schematically in Fig.2.

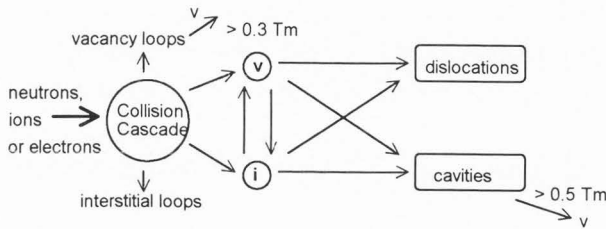


Figure 2. Schematic view of the basic components in the void growth mechanism

A considerable effort has been put into understanding the many facets of void formation and growth; a brief list, together with selected references is given in Table 1.

Table 1. Selected references relevant to the void growth mechanism.

Topic	References
Recoil spectra	Rehn and Okamoto, 1987, Zinkle and Singh, 1993
Cascade collapse	Averback, 1982, English and Jenkins, 1987
Diffusion in cascades	Mansur, Brailsford and Coghlan, 1987
Dislocation bias	Fastenau and Baskes, 1981
Void nucleation	Katz and Wiedersich, 1972, Singh and Foreman 1981
Void swelling theory	Harkness and Li, 1972, Brailsford and Bullough, 1978
Critical cavity radius	Townsend, 1982, Hishinuma and Mansur, 1983

In spite of the potential complexities, the heart of the void swelling mechanism is relatively straightforward. To illustrate this, we choose here to give the simplest rate equation approach to the void swelling mechanism. If vacancy loop effects, void shrinkage and recombination are ignored then the rate equations for vacancies and interstitials respectively are

$$K_v - D_v C_v (\alpha_c + \alpha_d) = 0 \quad (1)$$

$$K_i - D_i C_i (\alpha_c + Z_i \alpha_d) = 0 \quad (2)$$

where the K's, D's, C's and  $\alpha$ 's are production rates, diffusivities, concentrations and sink strengths, and  $Z_i$  is the dislocation bias for interstitials. The sink strength subscripts c and d refer to the cavity (void) and dislocations respectively. The rate of void swelling, S, per unit time, t, is equal to the net rate of arrival of vacancies at voids and is given by:

$$dS/dt = (D_v C_v - D_i C_i) \alpha_c \quad (3)$$

Substituting from equations 1 and 2 gives the swelling rate per displacement dose  $\phi$ , in terms of the dislocation bias, i.e.

$$\frac{dS}{d\phi} = \frac{Z_i - 1}{\{Y + Z_i + 1 + (Z_i/Y)\}} \quad (4)$$

where  $Y = (\alpha_c / \alpha_d)$  is the ratio of cavity to dislocation sink strength. In its simplest form for a dislocation density  $\rho$ , void radius r and void concentration C, this is given by

$$Y = 4\pi r C / \rho \quad (5)$$

A plot of void swelling rate against Y for  $Z_i = 1.01$  (or 10%) is shown in Fig.3 illustrating that the maximum swelling occurs when the void and dislocation sink strengths are almost equal (at  $Y = [Z_i]^{1/2}$ ), but that swelling is suppressed when either the void or dislocation sink dominates. This result led to the understanding of low bubble swelling in bcc metals, where normally high void densities are found, and to the effects of cold work in inhibiting swelling.

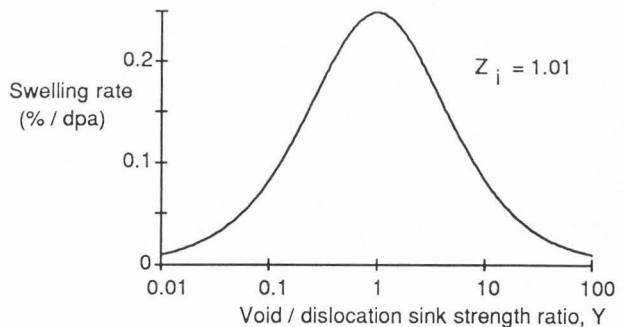


Figure 3. An example of the basic variation of void swelling with Y, the ratio of void and dislocation sink strengths

### Ion Implantation

Returning to the early days of void studies, an important step, particularly relevant to the title of this paper, was to recognise that ion implantation could be a very useful way of simulating the neutron damage. It was this simulation aspect that gave a large impetus to the use of ion beams to study void parameters in metals, the primary advantages with respect to reactor irradiations being the excellent control of important variables such as dose and temperature, the high

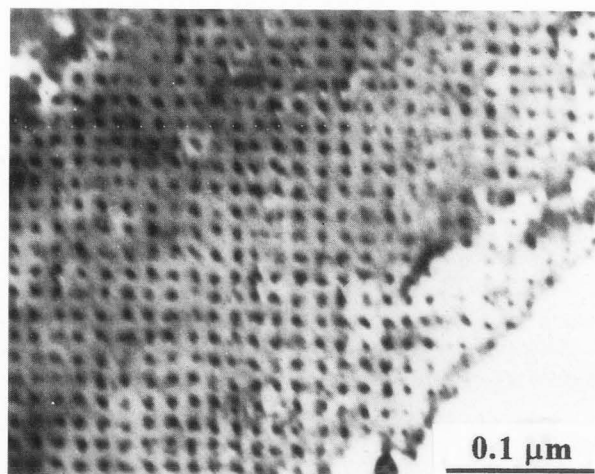


Figure 4. An example of the void lattice phenomenon showing alignment in ion implanted molybdenum viewed along the  $\langle 001 \rangle$  direction.

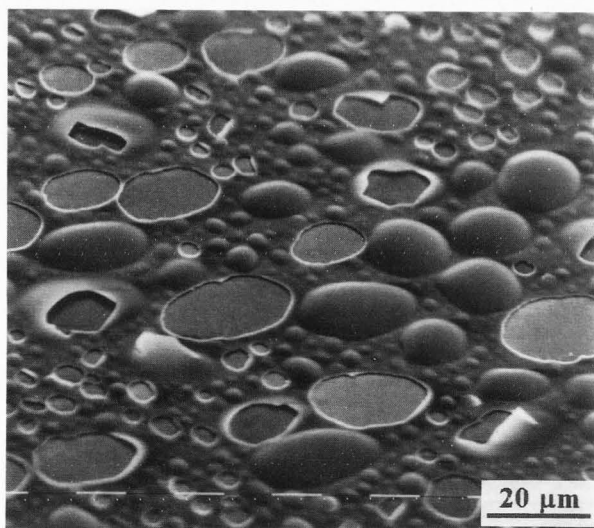


Figure 5. A scanning electron micrograph of helium ion induced blister formation on the surface of molybdenum.

displacement damage rates which allowed fast acquisition of relevant data, and the ease of sample handling. However, as emphasised by Mazey (1990) in a wide review of ion implantation simulation (including void growth studies), the correlation of ion and neutron damage can be non-trivial. Nevertheless, the contribution of ion beam studies to the detailed understanding of the many aspects of void swelling has been very positive.

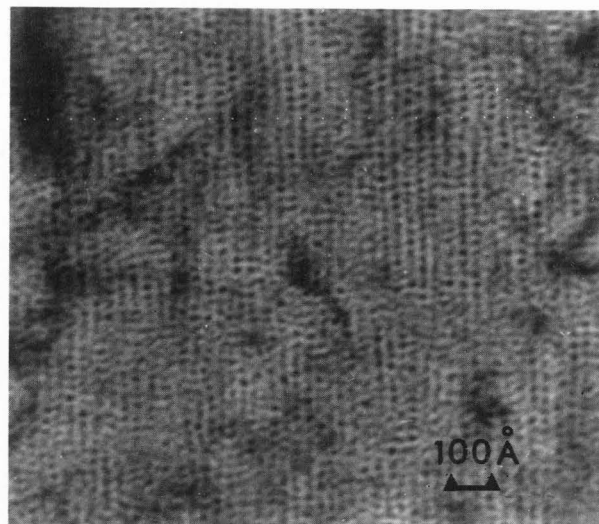


Figure 6. A TEM micrograph showing the high density of small helium bubbles, and a bubble lattice, in molybdenum after ion implantation at 300K.

#### Void Lattice Formation

One of the most unexpected observations in the early studies of void formation was the discovery of void lattice formation in molybdenum (Evans, 1971), with the aligned voids having the same bcc structure as the host metal, but with a lattice parameter some 100 times greater. An example is seen in Fig.4. Although the lattice was initially found in an ion beam experiment, its appearance in neutron irradiations studies followed very closely (Wiffen, 1972). Thus the phenomenon can be regarded as a good example of the use of ion beams to simulate the neutron environment. The void lattice turned out to appear far more frequently than could possibly have been predicted: not only was it subsequently found in other bcc metals (W, Ta, Nb), but also in fcc metals (Cu, Ni, Al) and hcp metals (Ti, Zr). Further studies showed that it was very easy to form lattices after helium ion implants in which bubble precipitation occurred (Johnson et al., 1983). Cavity ordering is also found in alumina, calcium fluoride and silicon. Early work is reviewed by Krishan (1982); this has been recently complemented by an update of both experimental and theoretical work (Evans, 1990).

As emphasised in the both reviews, all the lattices have the characteristic of being formed under displacement damage conditions. They are not formed or improved during annealing and not seen in helium bubble populations formed during tritium decay where no displacement damage is present. A second characteristic is that their structure is either identical to the host lattice (e.g. fcc in an fcc metal, bcc in a bcc metal) or closely related (e.g. parallel to the basal plane in hcp metals). Not surprisingly, there has been

much interest in providing an explanation for the phenomenon. Several proposals have suggested that the anisotropy of interstitial or interstitial loop movement, either in particular crystal directions or in particular crystal planes, is responsible (Foreman, 1972; Evans, 1987; Dubinko et al., 1989). As discussed in the work of Evans exploring the possible role of two dimensional interstitial migration, there is little doubt that this mechanism could apply in bcc and hcp metals. For the planar ordering in hcp metals, no other mechanism has been proposed but the situation is less clear in fcc metals. Here the model of Dubinko et al. (1989) using interstitial loops emitted from cascades could play a part. It is interesting that molecular dynamics studies of cascades have since shown this loop emission (Foreman et al., 1992). However, the mechanism cannot work for void lattice formation found under electron irradiation (Fisher and Williams, 1977) while its operation for bubble lattices has been questioned (Evans, 1990).

#### Bubble Growth During Inert Gas Implants

Interest in the area of bubble growth in metals has now been maintained over several decades. Early studies were inspired by their use as model systems for gas bubble behaviour in nuclear fuels, particularly  $\text{UO}_2$  where the need existed to understand the behaviour of the relatively large amounts of xenon and krypton formed in the fission process. However, although these early studies on metals used ion implantation (of helium in the MeV range) the concentrations involved were small, thus requiring annealing to investigate bubble behaviour (Barnes and Mazey, 1963). Nevertheless, many of the factors controlling annealing behaviour, such as gas bubble migration and coalescence, are also relevant in ion implantation experiments, at least if carried out at higher than moderate temperatures. Certainly, much of the physics of gas bubble behaviour in metals was put in place during these early studies (Blackburn, 1966).

The important step in studying inert gas behaviour in implanted material (i.e. without annealing) was the development of lower energy ion accelerators giving ion energies of the order of 100 keV. The compression of the implanted ion profiles with reduction in ion energy allowed high concentrations of inert gas atoms to be built up rapidly and gave the opportunity to uncover many interesting phenomena. Some of these will be discussed, roughly in chronological order, in the subsequent sections.

#### Helium Induced Blister Formation

The start of this large field of work can be traced back to Primak and Luthera (1966) who used interferometric and optical microscopy to demonstrate that as also found in non-metals, surface blisters were formed on copper and nickel after high doses of helium ions with energies between 40 and 140 keV. However,

relatively little work was carried out in this area until the early to mid-1970s when the combination of three factors, namely the availability of scanning electron microscopes, the similar availability of small accelerators and the sudden growth of interest in fusion reactor technology (where the potential of first wall erosion from the plasma constituents D,T and He was recognised (McCracken, 1975)), all contributed to a rapid resurgence in experimental studies.

The subsequent extensive investigations into helium induced blister formation have shown that the injection of mono-energetic helium ions into all metals (and many other solids) at ambient temperatures leads, at a critical dose, to the formation of surface blisters. A wide ranging review covering the many results up to 1983 has been written by Scherzer (1983). In Fig.5, we show a representative example of blisters formed on helium implanted molybdenum. The variations here with blister lids intact, broken or completely removed is typical. Complete surface flaking is also not infrequent.

Among the parameters affecting blister formation are the helium energy, ion dose, sample temperature and surface orientation but these can be rationalised to a large extent by the observation that blistering only occurs when the peak helium concentration in the deposited profile reaches about 30 at.%. The energy range of the helium ions used has been shown to be very wide, from 1 keV up to at least 3 MeV. At the lower end of this range, surface sputtering can suppress blister formation by preventing the build up of a sub-surface peak critical concentration.

With regard to the influence of the sample temperature, it emerged that unlike many physical phenomena, blister parameters were relatively insensitive to this parameter. Large changes only became apparent when temperatures approached about half the metal melting point when the morphology changed to one dominated by a pinhole or sponge like structure.

The association of blister formation with a high concentration of insoluble gas naturally suggested that the blister phenomenon was gas driven. However, to put the physical mechanism on a firmer footing, it was essential to gain some knowledge of the state of the helium in the metal. An important advance was the application of TEM techniques to examine the substructure in the regions of high helium concentration (Mazey et al., 1977). It emerged that consistently for doses near the critical dose and for temperatures below about  $0.4 T_m$ , samples contained very high concentrations ( $\sim 10^{25}/\text{m}^3$ ) of small bubbles with diameters in the 2 to 3 nm range. (This general result also holds for the implantation of the heavier inert gases discussed later, although bubble concentrations are somewhat lower). A micrograph illustrating helium bubbles in molybdenum is shown in Fig.6 where the additional feature of bubble lattice formation, as mentioned earlier, is also seen.

Although it might have been reasonable for the displacement damage vacancies to have played a role in bubble growth, this appeared to be inconsistent with the observations that neither the bubble structures or blister parameters changed noticeably over the range where vacancies became thermally mobile, e.g. Mo (Mazey et al., 1977). As a result, it was argued (Evans 1978) that the helium bubble growth in this range - and up to  $0.5 T_m$  - was independent of the displacement damage vacancies and grew instead by gas driven processes such as the loop punching process proposed by Greenwood et al., (1959). Such bubbles are therefore usually described as being overpressurised. The absence of any displacement damage influence when vacancies are mobile and the possibility of bias-driven growth must be present, has been discussed in more detail by Evans (1986). Even if helium is replaced by the heavier inert gas atoms where the displacement damage must be higher, this growth process is completely suppressed by the high bubble density dominated substructure - i.e. the value of  $Y$  in equations 4 and 5 is rather large with the consequent effects seen in Fig.3.

With these arguments for overpressurised bubbles, the mechanism of blister formation soon evolved: the continual growth of such bubbles must eventually put sufficient strain on the surrounding metal matrix to cause local microfracture of the metal. This process, termed interbubble fracture (Evans, 1978), must lead to sub-surface coalescence of bubbles along the maximum of the gas profile to give a large plate like bubble, parallel to the metal surface and eventual blister formation on the surface. The lack of blisters at high temperatures is then readily explained by the availability of thermal vacancies to maintain bubble equilibrium and prevent any overpressure.

As reviewed by Donnelly (1985), there was much subsequent interest in ascertaining the pressure in the helium bubbles and the associated gas packing densities within bubbles. The pressures are well beyond the range of validity of the van der Waals's equation so that interest in appropriate equations of state (EOS) was also initiated at this time. Returning to the mechanisms of bubble growth, the appearance of bubbles in metals charged with tritium (Thomas and Mintz, 1983) where the decay of tritium to helium-3 has no associated displacement damage, was clearly relevant. In addition, it appeared no coincidence that helium release and sample cracking took place at the same helium levels as that required for blister initiation (Evans, 1979). Other observations relevant to the bubble growth processes have been obtained from the technique of helium desorption spectrometry and from the so-called solid bubble observations. These will be treated in the following sections.

#### Helium Desorption Spectrometry

Helium desorption spectroscopy (HDS), in which gas release in implanted samples is measured during a linear temperature ramp, has provided unique

information about bubble nucleation processes and the growth of helium clusters. The central feature of this work has been the implantation of helium at low energies, 100 to 150 eV, to avoid any displacement damage, followed by a careful study of the size and temperature variations of desorption peaks with helium dose. Useful reviews on the numerous facets of the approach have been given by van Veen (1989, 1991). The relevant feature here has been the demonstration that a single vacancy will act as an unsaturable trap for incoming helium. Furthermore, in molybdenum and tungsten, up to 7 or 8 helium atoms can be bound to a vacancy while, crucially, additional helium leads to the formation of a Frenkel pair thereby allowing the helium trap to expand from a single vacancy to a divacancy. This process of converting a matrix atom to a self-interstitial, leaving space behind, can clearly be viewed as the first step of the loop punching process. Certainly, the HDS data indicates the process continues inexorably while when sufficient helium atoms have been added, TEM evidence of the loop punching process is very clear (Evans et al., 1981). The exact atomistic processes involved are not revealed in this work but interesting results are now available using the latest computer modelling techniques (Adams et al., 1991). It might be fair to add that while the process of loop punching can be demonstrated for isolated bubbles, the processes may be different in the more complex case when bubbles must clearly be very close and cooperative effects might not be unexpected.

#### Heavy Inert Gas Implants

Up to the mid-'80s, studies of bubble structures after implants of the heavier inert gases into metals were few and far between. However, this changed rapidly following the intriguing discovery by Templier et al., (1984) and vom Felde et al., (1984) that argon and xenon implanted into aluminium at ambient temperatures were precipitating within bubbles in the solid phase. Evans and Mazey (1985, 1986) extended this result to krypton in a number of metals and it became clear that the precipitates, conveniently described as 'solid bubbles', existed in the solid phase by virtue of the high pressures that resulted from the gas driven growth processes. It might be mentioned that the pressures necessary for the solidification of rare gases at 293K (from 0.4 GPa for xenon up to 4.7 GPa for neon) are well known from diamond anvil experiments (Finger et al., 1981).

One fortunate aspect was that the precipitates were usually found, at least in fcc, bcc and hcp metals to be epitaxially aligned with their close packed planes parallel to the close packed planes of the host metal. This behaviour has been shown by Finnis (1987) to be energetically favorable. A further result was that in fcc metals, the precipitates had an fcc structure, but were hcp in hcp metals. This is consistent with the known small energy difference between the two phases for rare gas solids. There was an important practical significance to this epitaxy since the precipitates then

gave easily detected reflections in electron diffraction rather than the rings expected from random orientation. An example is given in Fig. 7 for krypton in zirconium. Additional experimental features of interest are the dark field imaging of the solid precipitates, Moire fringe observations and heating experiments to follow precipitate melting.

One particular practical bonus in the solid bubble observations was that the lattice parameter, easily measured by comparison with the host matrix, gave a reasonable guide to bubble pressures when used with an appropriate equation of state. The pressures derived in this way gave values accurate enough to

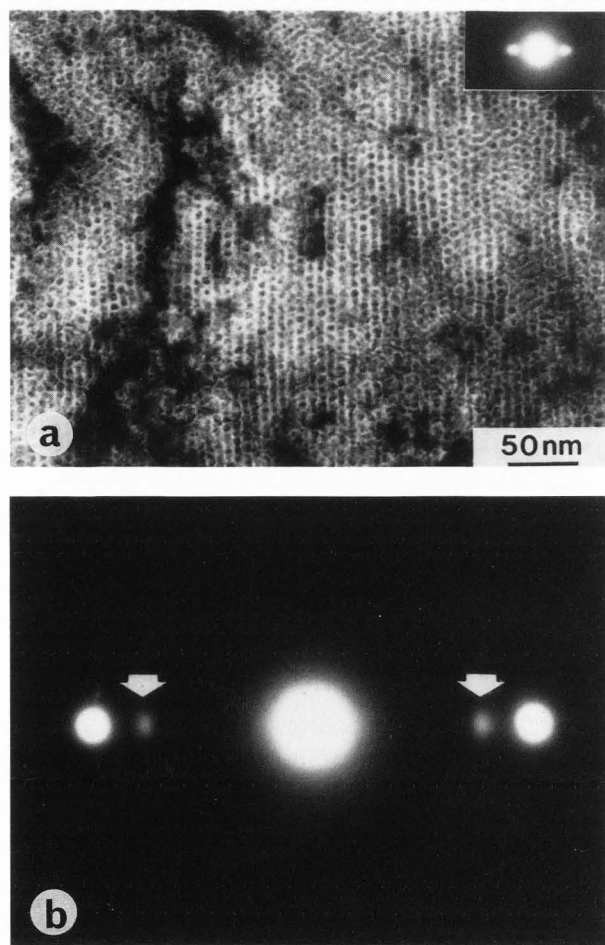


**Figure 7.** A TEM micrograph (a) and diffraction pattern (b) taken on krypton implanted zirconium. In (a), the high density of bubbles aligned in a two dimensional lattice parallel to the basal plane can be seen; in (b), the extra diffraction spots (arrowed) due to the solid krypton precipitates are visible. The diffraction spots in the inset are from the bubble lattice.

establish that bubble pressures drop during growth (Bircher and Liu, 1988) and that a good correlation exists between bubble pressures (ranging from 1 to 6 GPa) and the shear modulus of the host metal (Evans and Mazey, 1986). The correlation and its magnitude are consistent with the predictions of loop punching but while gas driven growth is generally accepted, the finer details are still open to discussion (Trinka, 1991, Donnelly et al., 1991).

#### Effects with other Ion Species

The description of gas driven bubble growth given earlier applies to cavities containing inert gas atoms, independent of whether the gas is in the solid or fluid phase. It was recognised (Evans, 1986) that the physics leading to the high pressures in the inert gas implants could also apply in other cases where the implanted species were insoluble and precipitation occurred. From the point of view of the metal, the space occupied by the precipitate must be viewed as a cavity and therefore precipitate growth must depend on vacancy acquisition, again by pressure driven processes. High pressure precipitates, possibly metastable, would not be unexpected in this description. An interesting possibility is whether carbon might, in an appropriate matrix, be persuaded to precipitate in the diamond phase.

#### High Temperature Effects

As already mentioned in relation to the formation of pinhole or sponge-like surfaces during high temperature helium implants, for ion implantations into metals at 0.5 Tm and above the dominating feature will be the influence of thermal vacancies in the lattice. These also influence bubble behaviour during annealing while the controlling equation is also relevant to high temperature void formation. For this equation, we again return to the important paper of Greenwood et al. (1959). There the rate equation governing the growth of a bubble with radius  $r$  and internal pressure  $P$  in material with atomic volume  $\Omega$  is given by

$$\frac{dr}{dt} = \frac{D_0}{r} \exp(-Q/kT) \{1 - \exp[-(P - 2\gamma/r)\Omega/kT]\} \quad (6)$$

where  $D_0$  and  $Q$  are the self-diffusion pre-exponential and activation energy,  $\gamma$  is surface energy,  $k$  is Boltzmann's constant and  $T$  is temperature. It is clear from this equation that the bubble growth is zero when the well known identity

$$P = 2\gamma/r \quad (7)$$

is satisfied, with growth or shrinkage when  $P$  is either greater or less than  $2\gamma/r$  respectively.

Returning for a moment to the void swelling situation, it can be seen that any void growth in this regime could be more than balanced by the void shrinkage rate. However, since voids usually contain the few gas atoms needed for nucleation, at very small sizes the pressure can be sufficient for equilibrium. In

the right temperature range, there can be an interesting balance between growth and shrinkage effects giving rise to the well known critical cavity radius concept for void nucleation (Hishinuma and Mansur, 1983)

One aspect that has received much less attention is the ability, under equilibrium conditions, for even small amounts of inert gas to give rise to significant material swelling. At any temperature the swelling due to inert gas atoms is given simply by the relation

$$S(\%) = G(\%).m \tag{8}$$

where G is gas content and m is the average no of vacancies/gas atom. In turn, we can write that m is equal to the total no of vacancies per unit volume,  $\rho_g$ , divided by the total no of gas atoms/unit vol,  $\rho_m$ ,

$$\text{i.e. } S(\%) = G(\%).\rho_m / \rho_g \tag{9}$$

For low gas pressures, the ideal gas law,  $PV = nkT$  is valid and can be rewritten as

$$P = \rho_g kT. \tag{10}$$

The bubble swelling is then given by

$$S(\%) = G(\%) \rho_m rkT/2\gamma \tag{11}$$

hence showing that for a given temperature and gas level, the key parameter is the (average) gas bubble radius. Although at ambient temperatures, ion implants give rise to bubbles of 2 or 3 nm diameter, for high temperature implants (or post irradiation annealing) bubble radii can be well into the micron range. The effect of this is shown in table 2 where the bubble swelling is calculated for different gas levels and different radii. In this example  $T = 1000K$ ,  $\gamma = 1 J/m^2$  and  $\rho_m = 6.5 \times 10^{22}/cm^3$ .

Table 2. Bubble swelling (%) as a function of gas content and bubble radius:

Bubble radius	Gas content (%)		
	10%	0.5%	0.01% (100ppm)
1nm	4.5	0.22	0.0045
10nm	45	2.25	0.045
0.1µm	450	22.5	0.45
1µm	-	225	4.5
10µm	-	-	45

The influence of the bubble radius can clearly be seen. In practice, the application of this simple approach to swelling levels is modified, particularly for high gas levels, by gas release effects. This is best known in  $UO_2$  where gas bubble accumulation at grain boundaries can lead to gross coalescence and the setting up of pathways, along boundaries, to the free surface where the gas is then lost (Tucker, 1980). However, as the table shows, and as has been shown

experimentally (Eldrup et al., 1991), even small amounts of inert gas can lead to very significant material swelling.

### Summary

It has been demonstrated that there are several modes of cavity growth under ion implantation. Cavities can be distinctly separated into voids and bubbles depending on whether the driving force for growth comes from displacement damage defects or from inert gas atoms. In addition, at high temperatures the behaviour of thermal vacancies imposes strong effects. For voids, shrinkage will occur but for bubbles, potentially large growth rates and associated swelling can take place. Within the framework of the growth processes, a number of interesting phenomena have been described. References to review papers have been emphasised to guide readers to more detailed accounts of these phenomena.

### References

- Adams JB, Wolfer WG, Foiles SM, Rohlfing CM, van Sicken CD (1991). Theoretical studies of helium in metals. Proc. NATO Advanced Research Workshop on Fundamental Aspects of Inert Gases in Solids, Bonas, France, Sept. 1990 (Eds. S.E. Donnelly and J.H. Evans), Plenum, New York and London, 3-16.
- Averback RS (1982). Ion irradiation studies of cascade damage in metals. J. Nucl. Mater. 108/109, 33-45
- Barnes RS, Mazey DJ (1963). The migration and coalescence of inert gas bubbles in metals. Proc. Royal Society 275, 47-57.
- Birtcher RC, Liu AS (1988). Temperature dependence of Kr precipitation in Ni. Mat. Res. Soc. Proc. 100, 225-230.
- Blackburn R (1966). Inert gases in metals. Metallurgical Reviews 11, 159-176.
- Brailsford AD and Bullough R (1978). Void growth and its relation to intrinsic point defect properties. J. Nucl. Mater. 69/70, 434-450.
- Cawthorne C, Fulton E (1966). Voids in irradiated stainless steel. Nature 216, 575-576.
- Corbett JW, Ianniello LC (Eds.) (1972). Proceedings of. Int. Conf. on Radiation Induced Voids in Metals, Albany, USA, USAEC, Oak Ridge, Symposium Series No 26.
- Diaz de la Rubia T, Guinan MW (1991). A new mechanism of defect production in metals: A molecular dynamics study of interstitial loop formation in high energy cascades, Phys.Rev. Letters 66, 2766-2769.
- Donnelly SE (1985). The density and pressure of helium in bubbles in implanted metals: a critical review. Radiation Effects 90, 1-47.
- Donnelly S, Mitchell DRG, van Veen A (1991). Loop punching as a mechanism for inert gas bubble growth in ion implanted metals. Proc. NATO Advanced Research Workshop on Fundamental Aspects of Inert Gases in Solids, Bonas, France, Sept.

1990 (Eds. S.E. Donnelly and J.H. Evans), Plenum, New York and London, 357-367.

Dubinko, VI, Tur AV, Turkin AA, Yanovskii VV (1989). A mechanism of formation and properties of the void lattice in metals under irradiation. *J. Nucl. Mater.* **161**, 57-71.

Eldrup M, Scov Pederson J, Horsewell A, Jensen KO, Evans JH (1991). Comparison of results from different experimental techniques (SANS, TEM, PAT, SEM) applied to bulk copper and nickel containing krypton. Proc. NATO Advanced Research Workshop on Fundamental Aspects of Inert Gases in Solids, Bonas, France, Sept. 1990 (Eds. S.E. Donnelly and J.H. Evans), Plenum, New York and London, 221-229.

English CA and Jenkins ML (1987). Insight into cascade collapse processes arising from studies of cascade collapse. Proc. Int. Conf. on Vacancies and Interstitials in Metals and Alloys, Berlin, Sept. 1986; *Materials Science Forum* 15-18, 1003-1022.

Evans JH (1971). Observations of a regular void array in high purity molybdenum and TZM irradiated at high temperatures with 2 MeV nitrogen ions. *Radiation Effects* **10**, 55-60.

Evans JH (1978). The role of implanted gas and lateral stress in blister formation mechanisms. Proc. Int. Conf. on Plasma Surface Interactions, Culham, April 1978, *J. Nucl. Mater.* **76/77**, 228-234.

Evans JH (1979). Helium behaviour in metals and metal tritides - some comparisons. *J. Nucl. Mater.* **79**, 249-251.

Evans JH, van Veen A, Caspers LM (1981). Direct evidence for helium bubble growth in molybdenum by the mechanism of loop punching. *Scripta Met.* **15**, 323-326.

Evans JH, Mazey DJ (1985). Evidence for solid krypton bubbles in copper, nickel and gold at 293K. *J. Phys. F* **15**, L1-L6.

Evans JH, Mazey DJ (1986). Solid bubble formation in titanium injected with krypton ions. *J. Nucl. Materials* **138**, 176-184.

Evans JH (1986). The formation of high pressure precipitation phases during the implantation of inert gas and other insoluble atom species in metals. *Nucl. Inst. and Methods B* **18**, 16-23.

Evans JH (1987). The role of two-dimensional self-interstitial diffusion in void lattice formation and other defect phenomena in metals. Proc. Int. Conf. on Vacancies and Interstitials in Metals and Alloys, Berlin, Sept. 1986; *Materials Science Forum* **15-18** (1987) 869-874.

Evans JH (1990). Irradiation-induced cavity lattice formation in materials. Proc. NATO Workshop on Patterns, Defects and Materials Instabilities (Eds. D. Walgraef and N.M. Ghoniem), Kluwer Academic Publishers, Dordrecht, Boston and London, 347-370.

Fastenau RHJ and Baskes MI (1981). Point defect - edge dislocation rate constants and bias factors. *J. Nucl. Mater.* **103/104**, 1421-1426.

Finger LW, Hazen RM, Zou G, Mao HK, Bell PM (1981). Structure and compression of crystalline

argon and neon at high pressure and room temperature. *Appl. Phys. Lett.* **39**, 892-894.

Finnis MW (1987). The role of the interface in determining the orientation of solid rare gas bubbles in metals. *Acta Metall.* **35**, 2543-2547.

Fisher SB, Williams KR (1977). Void spatial regularity in an electron irradiated stainless steel. *Radiation Effects* **32**, 123-124

Foreman AJE (1972). A mechanism for the formation of a regular void array in an irradiated metal. AERE Report 7135, Harwell Laboratory, UK, 1-9.

Foreman AJE, English CA, Phythian WJ (1992). Molecular dynamics calculations of displacement threshold energies and replacement collision sequences in copper using a many-body potential. *Phil. Mag. A* **66**, 655-669.

Greenwood GW, Foreman AJE, Rimmer DE (1959). The role of dislocations in the nucleation and growth of gas bubbles in irradiated fissile material. *J. Nucl. Mater.* **4**, 305-324.

Harkness SD and Li C-Y (1972). Theoretical study of the swelling of fast neutron irradiated materials. Proc. Int. Conf. on Radiation Induced Voids in Metals, Albany, (Eds. Corbett JW, Ianniello LC) USA, USAEC, Oak Ridge, Symposium Series No 26, 798-824.

Hishinuma A, Mansur LK (1983). Critical radius for bias driven swelling - A further analysis. *J. Nucl. Mater.* **118**, 91-99.

Ishino S, Kiritani M, Kondo T, Scott JL (Eds) (1991). Proceedings of 4th Int. Conf. on Fusion Reactor Materials, Kyoto, Japan, *J. Nucl. Mater.* **179-181**.

Johnson PB, Mazey DJ and Evans JH (1983). Bubble structures in helium irradiated metals. *Radiation Effects* **78**, 147-156.

Katz JL and Wiedersich H (1972). Nucleation of voids in materials during high energy irradiation. (1972). Proc. Int. Conf. on Radiation Induced Voids in Metals, Albany, (Eds. Corbett JW, Ianniello LC) USA, USAEC, Oak Ridge, Symposium Series No 26, 825-840.

Krishan K (1982). Ordering of voids and gas bubbles in radiation environments. *Radiation Effects* **66**, 121-155.

Loomis BA, Gerber SE, Taylor A (1977). Void ordering in ion irradiated niobium and tantalum, *J. Nucl. Mater.* **68**, 19-31.

Mansur LK, Brailsford AD and Coghlan WA (1987). Cascade diffusion theory of displacement induced point defect concentration and flux fluctuations. Proceedings. Int. Conference. on Vacancies and Interstitials in Metals and Alloys, Berlin, Sept. 1986; *Materials Science Forum* **15-18**, 1053-1062.

Mazey DJ, Eyre BL, Evans JH, Erents S, McCracken GM (1977). A transmission electron microscope study of molybdenum irradiated with helium ions. *J. Nucl. Mater.* **64**, 145-156.

- Mazey DJ (1990). Fundamental aspects of high energy ion beam simulation techniques and their relevance to fusion materials studies. *J. Nucl. Mater.* 174, 196-207.
- McCracken GM (1975). The behaviour of surfaces under ion bombardment. *Rep. Prog. Physics* 38, 241-327.
- Nygren RE, Gold RE, Jones RH (Eds.) (1981). Proceedings 2nd Topical Meeting on Fusion Reactor Materials, Seattle. *J. Nucl. Mater.* 103/104.
- Primak W, Luthera J (1966). Radiation blistering: Interferometric and microscopic observations of oxides, silicon and metals. *J. Applied Phys.* 37, 2287-2294.
- Pugh SF, Loretto MH, Norris DIR (Eds.) (1971). Proc. BNES Conference on Voids in Reactor Materials, Reading; British Nucl. Energy Society, London.
- Rehn LE and Okamoto PR (1987). Production of freely migrating defects during irradiation. *Proc. Int. Conf. on Vacancies and Interstitials in Metals and Alloys*, Berlin, Sept. 1986; *Materials Science Forum* 15-18, 985-1002.
- Scherzer BMU (1983). Development of surface topography due to gas ion implantation. *Topics in Applied Physics* Vol. 52 (Ed. R. Behrisch), Springer-Verlag, Berlin, pp. 271-355.
- Singh BN and Foreman AJE (1981). An assessment of void nucleation by gas atoms during irradiation. *J. Nuclear Materials.* 103/104, 1469-1474.
- Templier C, Jaouen C, Riviere J-P, Delafond J, Grilhe J (1984). Precipitation du xenon implante dans des alieges d'aluminium. (Precipitation of xenon implanted into aluminium foils). *Comptes.Rendus. Sc. Paris*, 299, 613-615.
- Thomas GJ, Mintz JM (1983). Helium bubbles in palladium tritide. *J. Nucl. Mater.* 116, 336-338.
- Townsend JR (1982). Critical cavity sizes in dual bombarded stainless steel: theoretical. *J. Nucl. Mater.* 108/109, 544-549.
- Trinkaus H (1991). Possible mechanisms limiting the pressure in inert gas bubbles in metals, *Proc. NATO Advanced Research Workshop on Fundamental Aspects of Inert Gases in Solids*, Bonas, France, Sept. 1990 (Eds. S.E. Donnelly and J.H. Evans), Plenum, New York and London, 369-383.
- Tucker MO (1980). Grain boundary porosity and gas release in irradiated UO<sub>2</sub>. *Rad. Effects* 53, 251-255.
- van Veen A (1989). Thermal vacancy desorption spectrometry as a tool for the study of vacancies and self-interstitials. *Proc. Int. Conf. on Vacancies and Interstitials in Metals and Alloys*, Berlin, Sept. 1986; *Materials Science Forum* 15-18, 3-24.
- van Veen A (1991) Helium-defect interactions in metals and silicon. *Proc. NATO Advanced Research Workshop on Fundamental Aspects of Inert Gases in Solids*, Bonas, France, Sept. 1990 (Eds. S.E. Donnelly and J.H. Evans), Plenum, New York & London, 41-57.
- vom Felde A, Fink J, Muller-Heinzinger Th, Pfluger J, Scheerer B, Linker G, and Kaletta D (1984). Pressure of neon, argon and xenon bubbles in aluminum. *Phys. Rev. Letters* 53, 922-925.
- Wiffen FW (1972). The effect of alloying and purity on the formation and ordering of voids in bcc metals. *Proc. Int. Conf. on Radiation Induced Voids in Metals*, Albany, USA, J.W. Corbett and L.C. Ianniello (Eds.); USAEC, Oak Ridge, Symposium Series No 26, 386-396.
- Woo CH and Singh BN (1992). Production bias due to clustering of point defects in irradiation induced cascades. *Phil. Mag. A* 65, 889-912.
- Zinkle SJ and Singh BN (1993). Analysis of displacement damage and defect production under cascade conditions. *J. Nucl. Mater.* 199, 173-191.

**Editor's Note:** All of the reviewer's concerns were appropriately addressed by text changes, hence there is no Discussion with Reviewers.